RSC Advances

ROYAL SOCIETY OF CHEMISTRY

www.rsc.org/advances

Journal Name

RSCPublishing

ARTICLE

Superhydrophobic hard nanofibers from soft matter

Cite this: DOI: 10.1039/x0xx00000x

Thierry Darmanin,[a] Claudio Mortier,[a] Julian Eastoe,[b] Masanobu Sagisaka,[c] and Frederic Guittard*[a]

Received 00th January 2012,
Accepted 00th January 2012

DOI: 10.1039/x0xx00000x

www.rsc.org/

Here, we show the possibility to change superhydrophobic properties from soft to hard polymer nanofibers by the control of the nature of branched molecules. In fact, we report the synthesis of original monomers derived from 3,4-ethylenedioxythiophene (ProDOT) and bearing two branched alkyl chains and their electrodeposition by cyclic voltammetry. We point out that hydrocarbon moiety (cheaper, available, non-toxic) can be an alternative to long fluorocarbon chains (expensive, from synthetic pathways, bioaccumulable) to reach anti-wetting properties. Moreover, we show that the change in the size of branched chains can change the surface morphology, from soft to hard nanofibers with an increase in the water adhesion due to a lower intrinsic hydrophobicity. Surprisingly, if these hard nanofibers can by generally obtained from inorganic chemistry, which are more resistance to lateral collapse and coalescence, we demonstrate the possibility to produce them from soft matter, i.e. polymers. In the case of the hard nanofibers, cross-section images reveal that these fibers are vertically aligned to the substrate. Moreover, we show that the height and the diameter of the hard nanofibers, as well as the distance between the fibers can be controlled by the number of deposition scans. Such materials could be used for many biomedical applications.

1. Introduction

Tuning the characteristics and hydrophilic/hydrophobic properties of nanofibers grown on surfaces is crucial for various applications such as cell,[1-2] protein[3-4] or bacteria adhesion,[5] tissue engineering,[6] membranes,[7] or encapsulation.[8] In the case of generation of superhydrophobicity, the wetting properties of surfaces[9-10] containing nanofibers highly depend on their intrinsic hydrophobicity, their characteristics (length, diameter), their orientation to the surface (horizontally, vertically) as well as the distance between them.[11] Hence, it is extremely important to find a way to control these characteristics.

Conducting polymers can be used to produce nanofibers.[12] While it was shown the possibility to produce nanofibers in solution,[13-17] it was also possible to induce the growth of nanofibers directly on substrates by self-assembly[18-23] or electrodeposition.[24-25] The electrodeposition process allows the control in the surface morphology simply by adjusting electrochemical parameters or by designing monomers. Various hydrophobic substituents can be grafted on the monomers to modify the intrinsic polymer hydrophobicity. For the growth of nanofibers, polyaniline,[26-27] polypyrrole,[28-30] poly(3,4-ethylenedioxythiophene) (PEDOT)[31-35] or poly(3,4-propylenedioxythiophene) (PProDOT)[36-38] derivatives have been described in the literature. One of the advantages of using ProDOT derivatives is the various possible positions for controlled substitution with hydrophobic substituents. Moreover, when ProDOT is substituted by two similar substituents in the 3-position, the possible configurations (head-to-head, tail-to-tail and head-to-tail) induced during the polymerization lead to the same polymer configuration, because the monomer is symmetric and does not contain an asymmetric carbon. As a consequence, the electrodeposited polymer is more ordered, which is also an advantage for the homogeneity of nanofiber growth. Another advantage is that the surface morphology is highly dependent on the nature of the substituent, and especially its intrinsic hydrophobicity. Hence, both fluorinated and alkyl chains have been used in the literature.[28-38] In the case of long fluorinated chains, our group is trying to replace them due to their bioaccumulative potential reported in animals and humans.[39-40] The high interactions between long fluorinated chains, their high insolubility and chemical resistance mean that they cannot be readily metabolized. Moreover, it is necessary that the hydrophobicity of the substituent is not too high in order to preserve the nanofiber morphology.[36a] To decrease the hydrophobicity of fluorinated or hydrocarbon chain, a way is to introduce branching, which decreases the interchain interactions. In the case of alkyl chains, linear alkyl chains were reported[35-36] but not branched alkyl chains.

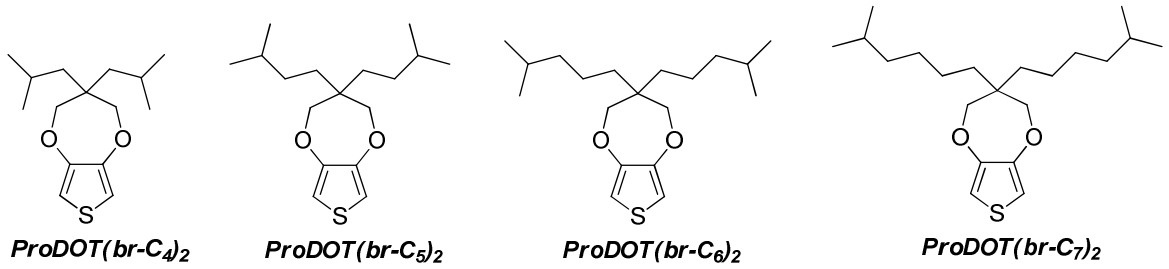

Scheme 1 Monomers synthesized in this work.

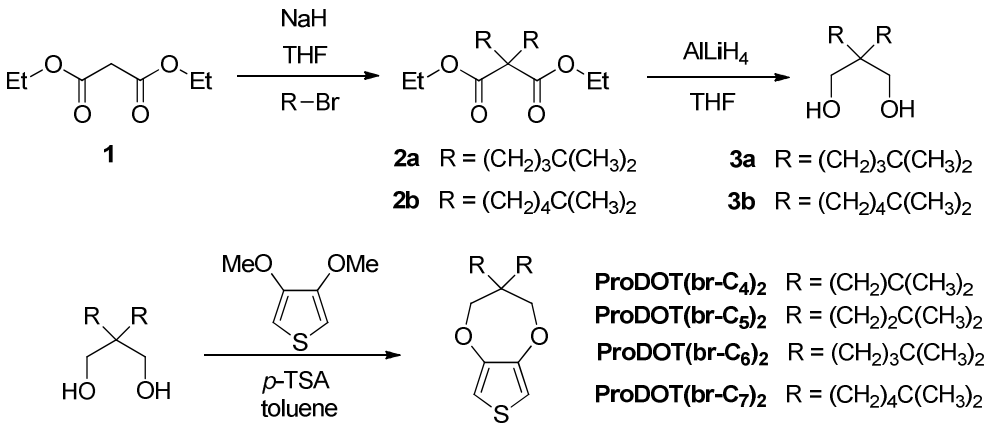

Scheme 2 Synthesis way to the monomers.

The interest to use branched alkyl chains has been clearly demonstrated for surfactants in solution[41-42] but not for surface of materials. Moreover, the branching of alkyl chains can also modify the properties of conducting polymers[43-44] and affect the surface morphology.

Here, the first study of electropolymerizible monomers with branched alkyl chains is reported. Four original ProDOT derivatives containing two branched alkyl chains have been synthesized, as represented in **Scheme 1** and Scheme 2, and the surface properties (wettability and morphology) of the corresponding electrodeposited polymers have been studied. It is shown how the size of the branched alkyl chains can be used to obtain soft and hard nanofibers.

2. Experimental

2.1 Monomer synthesis and characterization

The monomers were synthesized in four steps from diethyl malonate (1) and following the synthesis way represented in Scheme 2.

2,2-diisobutyl-1,3-propanediol and 2,2-diisopentyl-1,3-propanediol were purchased from TCI Europe N.V. The other diols (3a and 3b) were obtained by nucleophilic substitution of two hydrogen of diethyl malonate by the corresponding bromoalkane, and the reduction of the two ester groups with lithium aluminum hydride ($AlLiH_4$).[45] The general procedure is given below.

2.1.1. Synthesis of diethyl 2,2-bis(4-methylpentyl)malonate (2a) and diethyl 2,2-bis(5-methylhexyl)malonate (2b)

To 100 mL of anhydrous tetrahydrofuran (THF) containing 6 g of diethyl malonate (37 mmol), was added 2 g of sodium hydride (NaH) (90 mmol). After stirring for 15 min, the corresponding bromoalkane (90 mmol) was added and the mixture was refluxed for 24 h. Then, the solvent was removed and 100 mL of water were slowly added. The product was extracted with ethyl acetate, dried and the solvent removed by rotavapor and the product was finally distilled under vacuum.

Diethyl 2,2-bis(4-methylpentyl)malonate (2a).
Yield 25%; Colourless liquid; δ_H(200 MHz, $CDCl_3$, ppm): 4.16 (4 H, q, *J* 7.1), 1.83 (4 H, m), 1.54 (2 H, quint, 6.5), 1.23 (6 H, t, *J* 7.1), 1.16 (8 H, m), 0.84 (12 H, d, *J* 6.5).

Diethyl 2,2-bis(5-methylhexyl)malonate (2b).
Yield 20%; Colourless liquid; δ_H(200 MHz, $CDCl_3$, ppm): 4.16 (4 H, q, *J* 7.1), 1.85 (4 H, m), 1.50 (2 H, quint, *J* 6.6), 1.23 (6 H, t, *J* 7.1), 1.16 (12 H, m), 0.85 (12 H, d, *J* 6.6).

2.1.2. Synthesis of 2,2-bis(4-methylpentyl)propanediol (3a) and 2,2-bis(5-methylhexyl)propanediol (3b)

To 100 mL of anhydrous THF containing $AlLiH_4$ (30 mmol) was added dropwise the corresponding diol (13 mmol). After refluxing for 24 h, the reaction was quenched by addition of an aqueous saturated solution of potassium sodium tartrate. Then, the aluminum complexes were hydrolyzed with sulfuric acid and the extracted with ethyl acetate. After drying on Na_2SO_4 and solvent evaporation, the product was finally distilled under vacuum.

2,2-bis(4-methylpentyl)propanediol (3a).
Yield 95%; Colourless liquid; δ_H(200 MHz, $CDCl_3$, ppm): 3.58 (4 H, s), 2.05 (2 H, s), 1.55 (2 H, m), 1.21 (12 H, m), 0.87 (12 H, d, *J* 6.6).

2,2-bis(5-methylhexyl)propanediol (3b).
Yield 95%; Colourless liquid; δ_H(200 MHz, $CDCl_3$, ppm): 3.57 (s, 4H), 2.00 (s, 2H), 1.51 (m, 2H), 1.22 (m, 16H), 0.85 (d, $^3J_{HH}$ = 6.6 Hz, 12H).

2.1.3. Synthesis of monomers

Then, the monomers were synthesized by transetherification of 3,4-dimethoxythiophene with the corresponding 2,2-diisoalkyl-1,3-propanediol. To 40 mL of toluene containing 3,4-dimethoxythiophene (7 mmol) and sodium bisulphate (5 mmol) was added the corresponding diol (14 mmol). The solution was stirred at 95°C for 48 h. Then, the solvent was evaporated and the product purified by column chromatography (eluent: dichloromethane/cyclohexane 1:1).

3,3-diisobutyl-3,4-dihydro-2*H*-thieno[3,4-*b*][1,4]dioxepine (ProDOT(br-C_4)$_2$).
Yield 90%; Crystalline solid; m.p. 28.7°C; δ_H(200 MHz, $CDCl_3$, ppm): 6.42 (2 H, s), 3.93 (4 H, s), 1.77 (2 H, m), 1.42 (4 H, d, *J* 5.6), 0.96 (12 H, d, *J* 6.6); δ_C(200 MHz, $CDCl_3$, ppm): 149.67, 104.39, 78.27, 45.45, 42.26, 25.38, 23.39; FTIR (KBr): ν_{max}/cm^{-1} 3114, 2959, 2928, 2870, 1486, 1455, 1377, 1191, 1024; MS (70 eV): m/z 268 (M^+, 100), 155 ($C_7H_7O_2S^+$, 4), 141 ($C_6H_5O_2S^+$, 55), 127 ($C_4H_7OS^+$, 25), 116 ($C_4H_4O_2S^+$, 38).

3,3-diisopentyl-3,4-dihydro-2*H*-thieno[3,4-*b*][1,4]dioxepine (ProDOT(br-C_5)$_2$).
Yield 51%; Crystalline solid; m.p. 30.6°C; δ_H(200 MHz, $CDCl_3$, ppm): 6.42 (2 H, s), 3.84 (4 H, s), 1.49 (2 H, m), 1.38 (4 H, m), 1.12 (4 H, m), 1.03 (12 H, d, *J* 6.6); δ_C(200 MHz, $CDCl_3$, ppm): 149.70, 104.61, 77.58, 43.46, 31.66, 29.29, 28.74, 22.60; FTIR (KBr): ν_{max}/cm^{-1} 3111, 2955, 2928, 2866, 1484, 1455, 1375, 1189, 1020; MS (70 eV): m/z 296 (M^+, 100), 155 ($C_7H_7O_2S^+$, 4), 141 ($C_6H_5O_2S^+$, 15), 127 ($C_4H_7OS^+$, 10), 116 ($C_4H_4O_2S^+$, 30).

3,3-bis(4-methylpentyl)-3,4-dihydro-2*H*-thieno[3,4-*b*][1,4]dioxepine (ProDOT(br-C_6)$_2$).
Yield 44%; Colourless liquid; δ_H(200 MHz, $CDCl_3$, ppm): 6.42 (2 H, s), 3.85 (4 H, s), 1.55 (2 H, m), 1.25 (12 H, m), 0.87 (12 H, d, *J* 6.6); δ_C(200 MHz, $CDCl_3$, ppm): 149.71, 104.62, 77.49, 43.80, 39.73, 32.01, 27.75, 22.59, 20.49; FTIR (KBr): ν_{max}/cm^{-1} 3115, 2955, 2870, 1486, 1375, 1189, 1024; MS (70 eV): m/z 324 (M^+, 100), 155 ($C_7H_7O_2S^+$, 4), 141 ($C_6H_5O_2S^+$, 11), 127 ($C_4H_7OS^+$, 27), 116 ($C_4H_4O_2S^+$, 52).

3,3-bis(5-methylhexyl)-3,4-dihydro-2*H*-thieno[3,4-*b*][1,4]dioxepine (ProDOT(br-C_7)$_2$).
Yield 40%; Colourless liquid; δ_H(200 MHz, $CDCl_3$, ppm): 6.42 (2 H, s), 3.84 (4 H, s), 1.52 (12 H, m), 1.25 (16 H, m), 0.86 (12 H, d, *J* 6.6); δ_C(200 MHz, $CDCl_3$, ppm): 149.70, 104.64, 77.53, 43.72, 38.85, 31.87, 28.22, 27.96, 23.06, 22.61; FTIR (KBr): ν_{max}/cm^{-1} 3114, 2955, 2866, 1485, 1377, 1187, 1024; MS (70 eV): m/z 352 (M^+, 100), 155 ($C_7H_7O_2S^+$, 4), 141 ($C_6H_5O_2S^+$, 17), 127 ($C_4H_7OS^+$, 22), 116 ($C_4H_4O_2S^+$, 49).

2.2. Electropolymerization

Gold plates (deposition of 20 nm chromium and 150 nm gold on silicon wafer) were purchased from Neyco. The electropolymerization process consisted in a three-electrode system: a gold plate as working electrode, a glassy carbon rod as counter-electrode and a saturated calomel reference electrode (SCE). The three-electrode system was connected to an Autolab potentiostat (Metrohm). The electrodes were inserted in a glass cell, in which 10 mL of anhydrous acetonitrile containing 0.1 M of tetrabutylammonium perchlorate (Bu_4NClO_4) and 0.01 M of monomer were added. The solution was, then, degassed with argon. The monomer oxidation potential was determined by cyclic voltammetry (E^{ox} = 1.52-1.59 V *vs* SCE following the monomer used). Then, cyclic voltammetry was used as the deposition method because it induced the formation of highly homogenous films with high adhesion. With this method, one, three and five scans were performed and with a scan rate of 20 mV s^{-1}. An example of cyclic voltammogram is given in Figure 1.

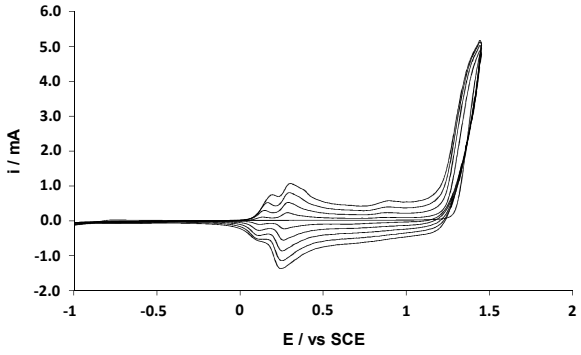

Fig. 1 Cyclic voltammogram of ProDOT(br-C_6)$_2$ (0.01 M) recorded in anhydrous acetonitrile containing 0.1 M of Bu_4NClO_4; Scan rate: 20 mV s^{-1}; Number of scans: 5.

2.3. Surface characterization

The surface morphology was investigated by scanning electron microscopy (SEM) using a 6700F microscope (JEOL). The hydrophobicity of the polymer films was investigated by water

contact angle measurements using a DSA30 goniometer (Krüss). The static contact angles were obtained with the sessile drop method, whereas the dynamic contact angles were obtained with the tilted-drop method. Using this last method, the advanced and receding contact angles, and as a consequence the hysteresis (H), were determined after surface inclination and just before the water droplets roll off the surface. The maximum surface inclination is called sliding angle (α).

3. Results and Discussion

3.1 Surface hydrophobicity

The polymers were electrodeposited by cyclic voltammetry because it induced the formation of highly homogenous films with high adhesion. With this method, one, three and five scans were performed and with a scan rate of 20 mV s^{-1}. In this process, the polymers are obtained in their reduced state (uncharged).

The best results were obtained for three deposition scans. For three deposition scans, the apparent contact angles of water (θ_w) as a function of the number of carbons in the branched alkyl chains (n) are displayed on Figure 2A. This graph shows that PProDOT(br-C_4)$_2$, PProDOT(br-C_6)$_2$ and PProDOT(br-C_7)$_2$ were superhydrophobic with $\theta_w > 150°$, but a lower value was obtained for PProDOT(br-C_5)$_2$ (θ_w = 136.8°). Moreover, dynamic contact angle measurements showed very low hysteresis (H) and sliding angles (α) for PProDOT(br-C_6)$_2$ (H = 5.0° and α = 5.0°) and PProDOT(br-C_7)$_2$ (H = 5.7° and α = 4.7°). In an opposite manner, water droplets deposited on PProDOT(br-C_4)$_2$ and PProDOT(br-C_5)$_2$ remained stuck even after surface inclination of 90° revealing a very high adhesion. To explain these phenomena it was first necessary to explore the surface morphologies.

3.2. Surface morphology

Figure 3 gathers the SEM images of each polymers for three deposition scans. A very unexpected change in the surface morphology was observed from hard polymer nanofibers for PProDOT(br-C_4)$_2$ to soft polymer nanofibers for PProDOT(br-C_6)$_2$ and PProDOT(br-C_7)$_2$. Here, hard nanofibers can be considered as nanoneedles while soft nanofibers are fibers with highly curved surfaces. The change was observed for PProDOT(br-C_5)$_2$, for which the surface was not highly structured explaining the lower value of θ_w obtained for this polymer. Here, the unexpected result was to obtain hard nanofibers because the polymers are considered as soft materials in comparison to metals and inorganic materials. Indeed, it is extremely difficult to elaborate vertically aligned polymer nanofibers because of their lateral collapse and coalescence, for example during evaporation, due to capillary forces and low stiffness of the fibers.[46-49]

Such fibers were never observed by electrodeposition even with linear alkyl chains,[35-36] which shows an effect of the use of branched alkyl chains to control the hardness of nanofibers. Moreover, the hard nanofibers were vertically aligned to the substrate, which could affect the surface wettability.

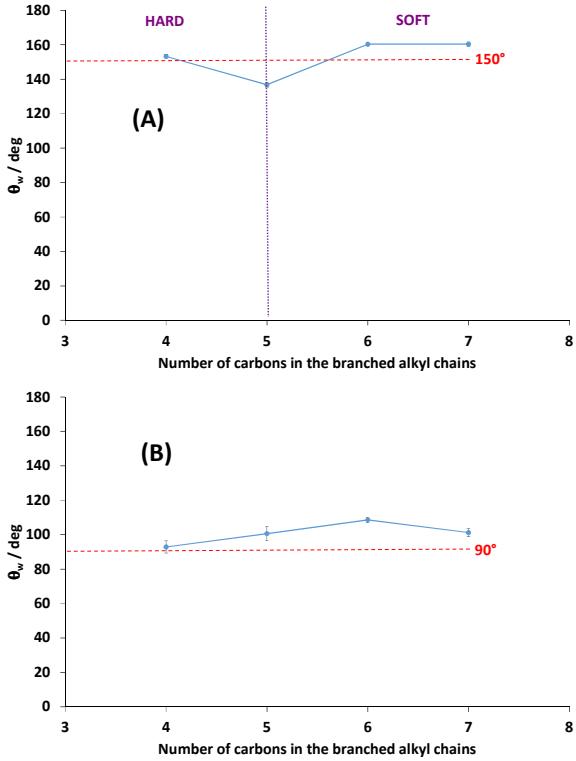

Fig. 2 Apparent contact angle of water (θ_w) as a function of the number of carbons in the branched alkyl chains for (A) the structured (3 scans by cyclic voltammetry at 20 mV s^{-1}) and (B) the corresponding smooth films (1 mC cm^{-2} at imposed potential).

Now, it is now possible to explain the results for surface properties in terms of the Wenzel and Cassie-Baxter equations.[50-51] Indeed, these two equations can be used to explain superhydrophobic properties but with different adhesions. In the Wenzel state[50] ($\cos\theta = r\cos\theta^Y$ with r a roughness parameter and θ^Y the Young angle),[52] a water droplet is in full contact with the surface. As a consequence, the presence of surface roughness can lead to superhydrophobic properties if the materials are intrinsically hydrophobic ($\theta^Y > 90°$) and reversely. However, the increase in the solid-liquid interface with the surface roughness also induces an increase in H, leading to superhydrophobic properties but with high adhesion. When the surface is rough but also porous, a water droplet can be in the Cassie-Baxter state:[51] $\cos\theta = f\cos\theta^Y + f - 1$ with f the solid fraction and (1 – f) the air fraction. A water droplet sits on top on the surface roughness but also on air pockets entrapped between the solid and the surface. Here, a surface can be superhydrophobic whatever θ^Y if the surface morphology favors the Cassie-Baxter state. Moreover, in the Cassie-Baxter state the adhesion of water is extremely low due to the presence of air, which induces the presence of a liquid-vapor interface.

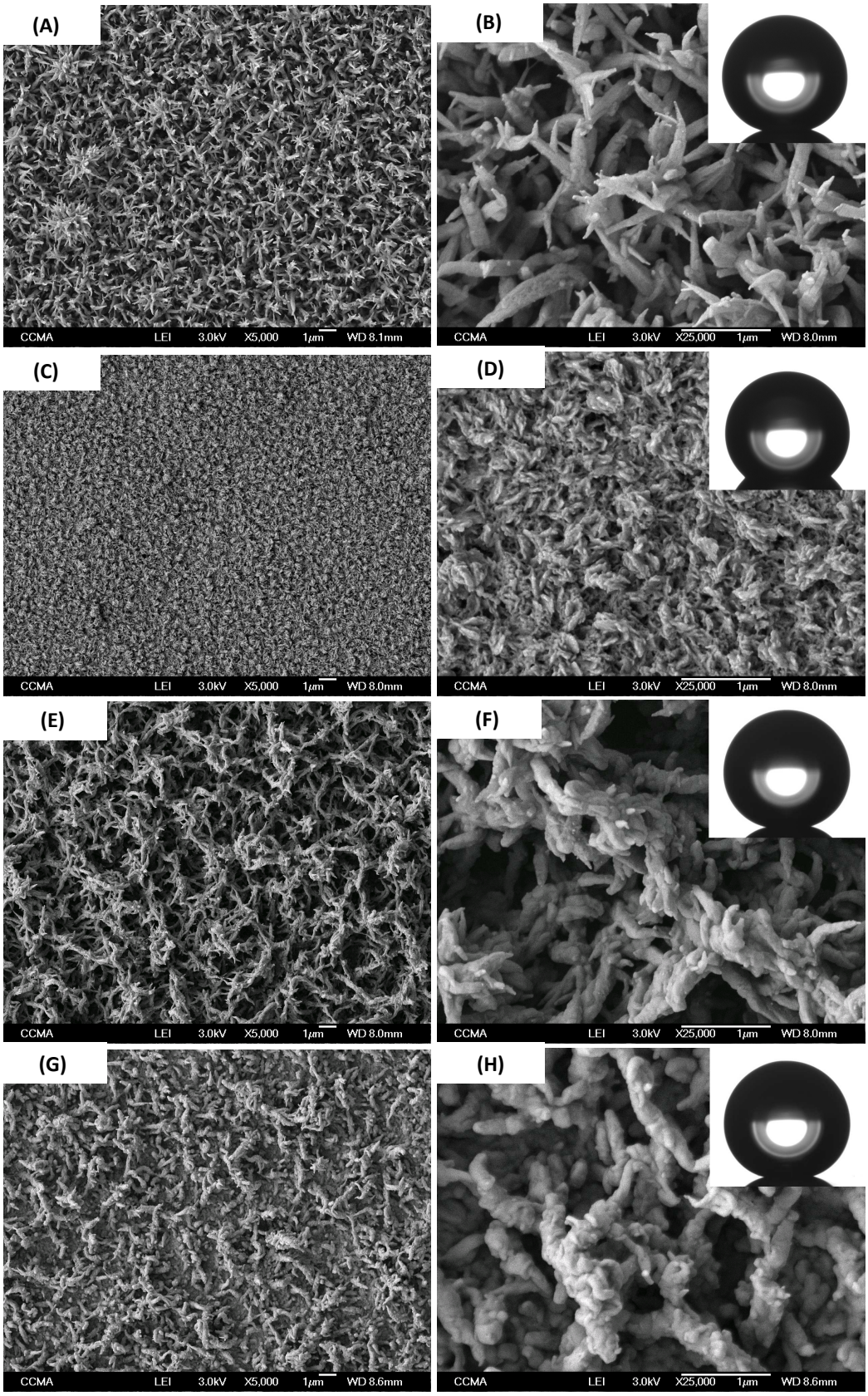

Fig. 3 SEM images of the polymers at two magnifications (x 5000 and x 25000): (A,B) PProDOT(br-C_4)$_2$, (C,D) PProDOT(br-C_5)$_2$, (E,F) PProDOT(br-C_6)$_2$, (G,H) PProDOT(br-C_7)$_2$; number of scans: 3. The insets represent picture of water droplet on the surfaces.

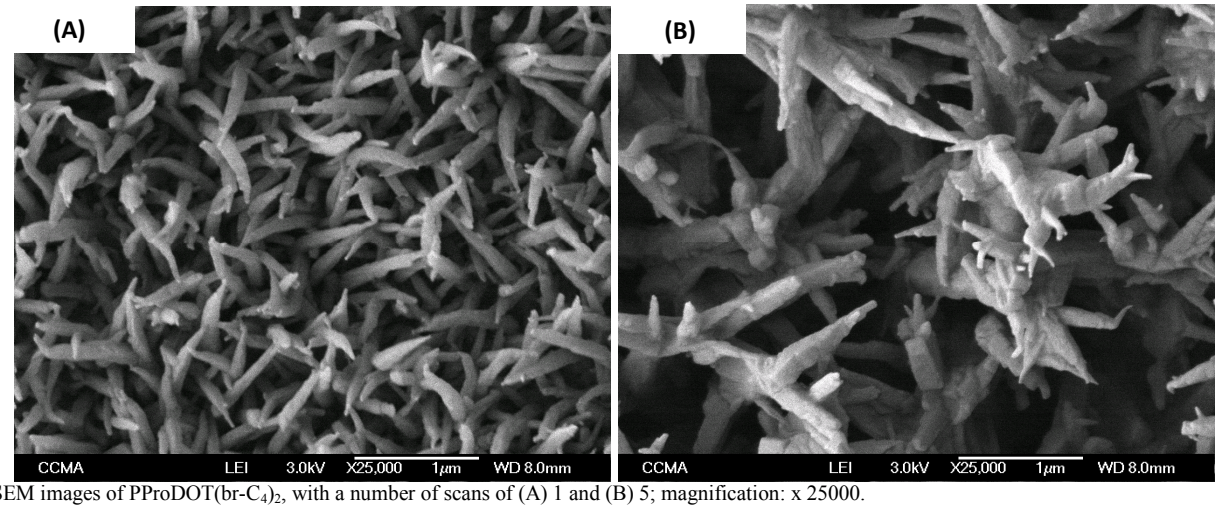

Fig. 6 SEM images of PProDOT(br-C_4)$_2$, with a number of scans of (A) 1 and (B) 5; magnification: x 25000.

Because the Wenzel and Cassie-Baxter equation are depending on θ^Y, it was first necessary to determine these angles by producing smooth surfaces for each polymer. Here, it was possible to obtain smooth films for each polymer by changing the deposition process, and using a deposition at constant potential. Smooth surfaces were obtained using an extremely low deposition charge (Qs = 1 mC cm^{-2}) allowing to cover the substrate without formation of structures. However, to obtain the same polymer, a reduction step by cyclic voltammetry (one back scan from 0.8 V to -0.5 V at 20 mV s^{-1}) was added after the deposition to reduce the polymer. The smoothness of the surfaces was confirmed by determining the surface roughness using an optical profilometry (Table1 and Figure 4). Their mean roughness (Ra) was below 10 nm and was quite the same for each polymer. Figure 2B shows the apparent contact angles obtained on the smooth surfaces. An increase of θ^Y was observed between PProDOT(br-C_4)$_2$ and PProDOT(br-C_6)$_2$ and a decrease after, which means that for PProDOT(br-C_7)$_2$ the surface is saturated by hydrocarbon chains. Moreover, PProDOT(br-C_5)$_2$, PProDOT(br-C_6)$_2$ and PProDOT(br-C_7)$_2$ are intrinsically hydrophobic ($\theta^Y > 90°$), whereas for PProDOT(br-C_4)$_2$ θ^Y was close to 90°. Now the results can be explained with the Wenzel and Cassie-Baxter equation. In the case of PProDOT(br-C_6)$_2$ and PProDOT(br-C_7)$_2$, water droplets deposited on these surfaces were close to the Cassie-Baxter state (low H and α) because of their intrinsic hydrophobicity and because the presence of the nanofibers allow to trap a high amount of air between the droplets and the surface.

Table 1 Roughness parameters of the "smooth" polymers

Polymer	Ra [nm]	Rq [nm]
PProDOT(br-C_4)$_2$	9.3	11.9
PProDOT(br-C_5)$_2$	9.1	11.5
PProDOT(br-C_6)$_2$	9.5	11.9
PProDOT(br-C_7)$_2$	9.2	11.7

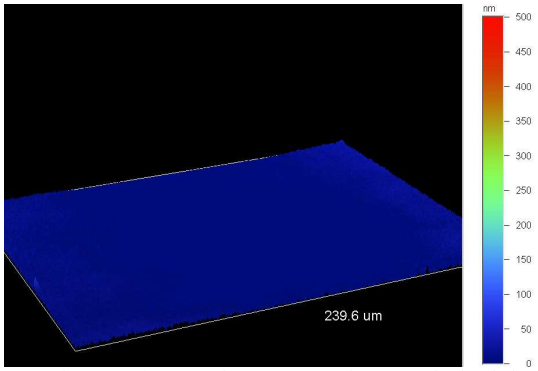

Fig. 4 3-D image of "smooth" PProDOT(br-C_7)$_2$ obtained by optical profilometry.

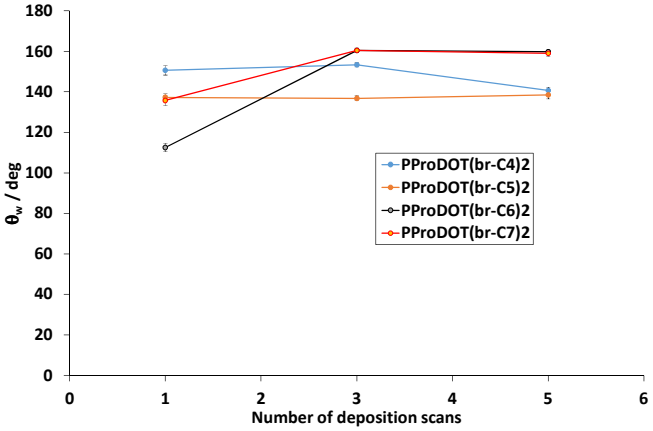

Fig. 5 Apparent water contact angles of the polymers as a function of the deposition charge.

For PProDOT(br-C_5)$_2$, the high hydrophobicity and high adhesion can be explained with the Wenzel equation because the surface is not highly structured and θ^Y is > 90°.

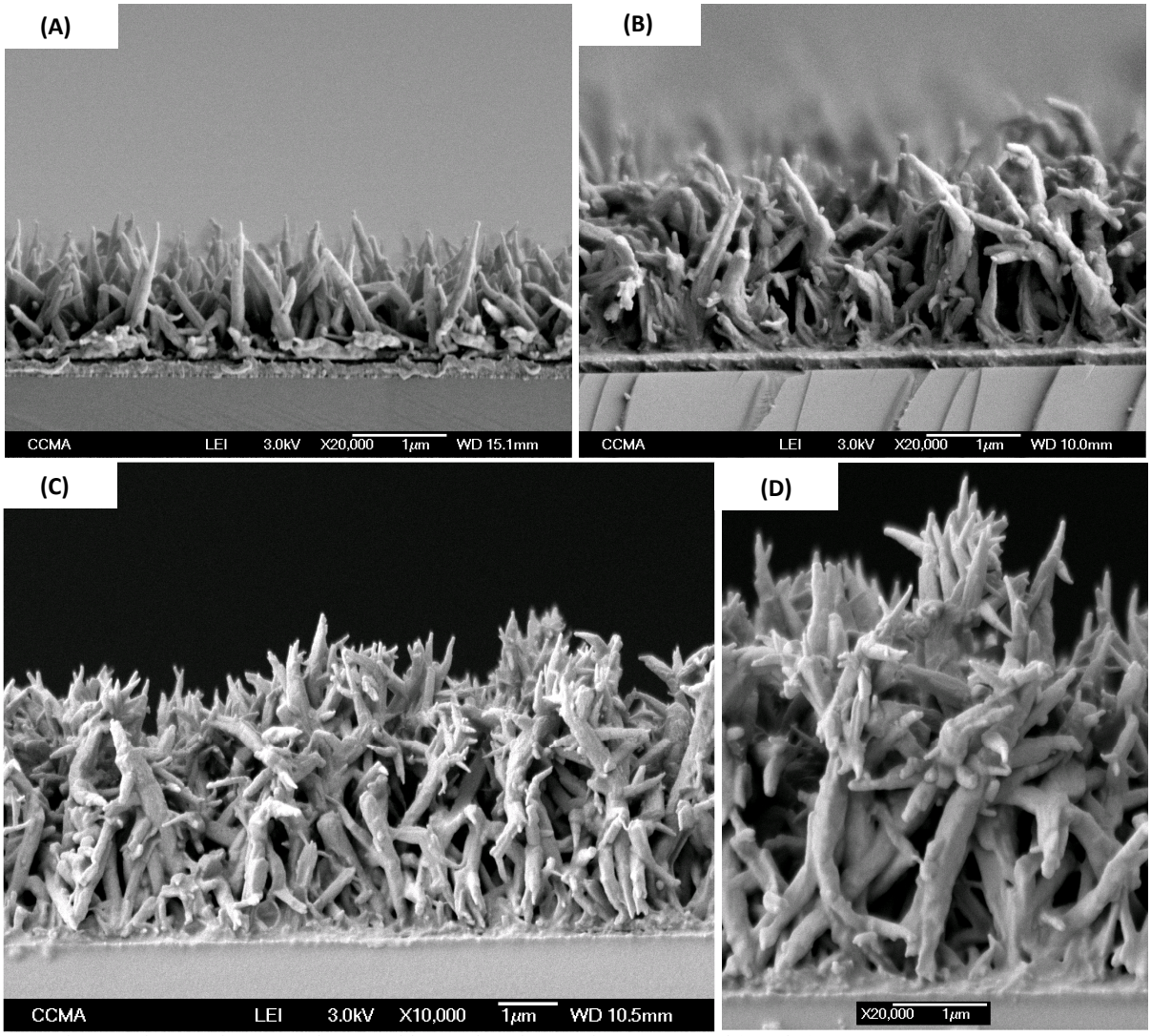

Fig. 7 Cross-section SEM images of PProDOT(br-C_4)$_2$, with a number of scans of (A) 1, (B) 3 and (C and D) 5.

For PProDOT(br-C_5)$_2$, θ_w was above 150° but the adhesion of water is extremely high. However, this state cannot be explained with the Wenzel equation because θ^Y is close to 90° (if $\theta^Y = 90°$, the surface roughness has not effect on the surface hydrophobicity). Indeed, if the presence of the hard nanofibers can favor the Cassie-Baxter state, the lower θ^Y increases the water penetration inside the roughness. Here, the water droplet was probably in an intermediate state between the Wenzel and the Cassie-Baxter known as an impregnating Cassie-Baxter state (Cassie-Baxter state with high adhesion), as observed on the surface of red roses.[53-55] Their surface adhesion if due to the combination of microstructures called micropapillae of 16 μm in diameter and 7 μm in height, which are covered by nanofolds. Similar adhesion properties were also reported for the peanut leaves.[56] In the literature, this state is often called "sticky superhydrophobicity" and Marmur proposed to use the term parahydrophobicity.[57] This state can be predicted using the Cassie-Baxter equation and with multivalued roughness topographies such as overhangs, re-entrant structures, T-like structures or mushroom-like structures.[58] Indeed, the air trapped below multivalued roughness topographies can induce a negative Laplace pressure difference changing the liquid−vapor interface and impeding the liquid penetration.[59] It is possible to control the liquid penetration inside the roughness and have various adhesions by playing with the geometrical parameters of the multivalued roughness topographies. Bormashenko and Starov also studied the liquid penetration inside capillaries of different sizes.[60] They showed that small capillarities promote the Wenzel state while large capillarities favor the Cassie-Baxter state. In our case, for PProDOT(br-C_4)$_2$, the presence of the nanofibers as well as their low intrinsic hydrophobicity favored the Cassie-Baxter state but with an important liquid penetration inside the roughness, which led to a high water adhesion.

3.3. Influence of the number of deposition scans

Hence, due to the presence of the hard nanofibers, PProDOT(br-C_4)$_2$ was chosen to study the influence of the number of scans on the surface hydrophobicity and morphology. The influence of the number of scans on the surface hydrophobicity is represented in Figure 5. Hence, similar hydrophobicities were obtained for one to three scans, whereas a decrease in θ_w was observed for five scans. Moreover, PProDOT(br-C_4)$_2$ was always sticky whatever the number of scans. The SEM images are given in Figures 6. An increase in the characteristics of the nanofibers (diameter and length) was observed as a function of the numbers of scans.

As a consequence, the growth is not only in one dimension but is two-dimensional. To have more information, cross-section images were also performed as shown in Figure 7. This figure confirms the vertical alignment of the nanofibers and the increase in the diameter and length with scan number. Moreover, for only one scan, most of the fibers were linear (Figure 6A), but inclination angles were present after as shown in Figure 7B. For five scans (Figure 7C and 7D), the distance between the fibers seemed to be too important which may explain the decrease in θ_w.

4. Conclusions

Here, we have reported the synthesis and characterization of original ProDOT monomers containing branched alkyl chains for the elaboration of superhydrophobic films by cyclic voltammetry electrodeposition. These molecules pointed out that hydrocarbon derivatives (cheaper, available feed stock, non-toxic) can be an alternative to long fluorocarbon chains (expensive, from synthetic pathway, bioaccumulable) to reach anti-wetting properties. Surprisingly, the control of molecular shape and their electrodeposition could lead from superhydrophobic soft to hard nanofibers. In fact, these hard nanofibers are generally obtained from inorganic materials, which are more resistant to lateral collapse and coalescence. Here, we demonstrated the possibility to obtain these fibers from soft matter (i.e. polymers). In this case, the decrease in the size of branched chains allowed to change the morphology from soft to hard nanofibers with an increase in the water adhesion due to a lower intrinsic hydrophobicity. Moreover, in the case of the hard nanofibers, cross-section images revealed the vertical alignment of these fibers to the substrate. Furthermore, it was possible to control the height and the diameter of the hard nanofibers, as well as the distance between the fibers by the number the deposition scans. Such nanofibrous materials are extremely interesting and could be used for various biomedical applications such as in tissue engineering, biosensors or anti-bioadhesion. The branched molecules can be a new vision in material chemistry to build-up superhydrophobic nanofibers.

Notes and references

[a] *Univ. Nice Sophia Antipolis, LPMC, UMR 7336, CNRS, Parc Valrose, 06100 Nice, France*
Fax: (+33)4-92-07-61-56; Tel: (+33)4-92-07-61-59;
E-mail:Frederic.GUITTARD@unice.fr

[b]School of Chemistry, University of Bristol, Bristol, BS8 1TS, UK

[c]Department of Frontier Materials Chemistry, Graduate School of Science and Technology, Hirosaki University, Japan

1 Y. Lai, L. Lin, F. Pan, J. Huang, R. Song, Y. Huang, C. Lin, H. Fuchs and L. Chi, *Small*, 2013, **9**, 2945.
2 K. H. Lee, G. H. Kwon, S. J. Shin, J.-Y. Baek, D. K. Han, Y. Park and S. H. Lee, *J. Biomed. Mater. Res., Part A*, 2008, **90**, 619.
3 M. J. Pérez-Roldan, A. Parracino, G. Ceccone, P. Colpo and F. Rossi, *Plasma Processes Polym.*, 2014, **11**, 577.
4 F.-q. Sun, X.-s. Li, J.-k. Xu and P.t. Cao, *Chin. J. Polym. Sci.*, 2010, **28**, 705.
5 J. Tarrade, T. Darmanin, E. Taffin de Givenchy, F. Guittard, D. Debarnot and F. Poncin-Epaillard, *Appl. Surf. Sci.*, 2014, **292**, 782.
6 K. E. Park, K. Y. Lee, S. J. Lee and W. H. Park, *Macromol. Symp.*, 2007, **249-250**, 103.
7 N.-N. Bui, and J. R. McCutcheon, *Environ. Sci. Technol.*, 2013, **47**, 1761.
8 J. E. Díaz, A. Barrero, M. Márquez and I. G. Loscertales, *Adv. Funct. Mater.*, 2006, **16**, 2110.
9 H. Bellanger, T. Darmanin, E. Taffin de Givenchy and F. Guittard, *Chem. Rev.*, 2014, **114**, 2694.
10 E. Celia, T. Darmanin, E. Taffin de Givenchy, S. Amigoni and F. Guittard, *J. Colloid Interface Sci.*, 2013, **402**, 1.
11 M. Wolfs, T. Darmanin and F. Guittard, *Polym. Rev.*, 2013, **53**, 460.
12 T. Darmanin and F. Guittard, *Prog. Polym. Sci.*, 2014, **39**, 656.
13 W. Zhong, S. Liu, X. Chen, Y. Wang and W. Yang, 2006, **39**, 3224.
14 Y. Zhu, D. Hu, M. Wan, L. Jiang and Y. Wie, *Adv. Mater.*, 2007, **19**, 2092.
15 H. Fan, H. Wang, J. Guo, N. Zhao, and J. Xu, *J. Colloid Interface Sci.*, 2013, **409**, 255.
16 Y. Zhu, J. Li, M. Wan and L. Jiang, *Macromol. Rapid Commun.*, 2008, **29**, 239.
17 J. Wang, J. Wang, Z. Wang and F. Zhang, *Macromol. Rapid Commun.*, 2009, **30**, 604.
18 N.-R. Chiou, C. Lu, J. Guan, L. J. Lee and A. J. Epstein, *Nat. Nanotechnol.*, 2007, **2**, 354.
19 S. B. Kulkarni, S. S. Joshi and C. D. Lokhande, *Chem. Eng. J.*, 2011, **166**, 1179.
20 H. Zhou, Z. Shi and Y. Lu, *Synth. Met.*, 2010, **160**, 1925.
21 J. Yan, X. Han, J. He, L. Kang, B. Zhang, Y. Du, H. Zhao, C. Dong, H. L. Wang and P. Xu, *ACS Appl. Mater. Interfaces*, 2012, **4**, 2752.
22 P. Xu, N. H. Mack, S. H. Jeon, S. K. Doorn, X. Han and H. L. Wang, *Langmuir*, 2010, **26**, 8882.
23 Y. Zhu, J. Li, H. He, M. Wan and L. Jiang, *Macromol. Rapid Commun.*, 2007, **28**, 2230.
24 T. Darmanin, E. Taffin de Givenchy, S. Amigoni and F. Guittard, *Adv. Mater.*, 2013, **25**, 1378.

25 T. Darmanin and F. Guittard, *J. Am. Chem. Soc.*, 2009, **131**, 7928.
26 L. Xu, Z. Chen, W. Chen, A. Mulchandani and Y. Yan, *Macromol. Rapid Commun.*, 2008, **29**, 832.
27 H. Zhang, J. Wang, Z. Zhou, Z. Wang, F. Zhang and S. Wang, *Macromol. Rapid Commun.*, 2008, **29**, 68.
28 H. Yan, K. Kurogi, H. Mayama and K. Tsujii, *Angew. Chem., Int. Ed.*, 2005, **44**, 3453.
29 J. Zang, C. M. Li, S. J. Bao, X. Cui, Q. Bao and C. Q. Sun, *Macromolecules*, 2008, **41**, 7053.
30 C. Ding, Y. Zhu, M. Liu, L. Feng, M. Wan and L. Jiang, L. *Soft Matter*, 2012, **8**, 9064.
31 a) S.-C. Luo, J. Sekine, B. Zhu, H. Zhao, A. Nakao and H.-h. Yu, *ACS Nano*, 2012, **6**, 3018; b) S.-C. Luo, S.S. Liour and H.-h. Yu, *Chem. Commun.*, 2010, **46**, 4731.
32 M. Wolfs, T. Darmanin and F. Guittard, F. *Soft Matter*, 2012, **8**, 9110.
33 P. Conte, T. Darmanin and F. Guittard, *React. Funct. Polym.*, 2014, **74**, 46.
34 T. Darmanin and F. Guittard, *J. Am. Chem. Soc.*, 2011, **133**, 15627.
35 O. Dunand, T. Darmanin and F. Guittard, *ChemPhysChem*, 2013, **14**, 2947.
36 a) M. Wolfs, T. Darmanin and F. Guittard, *RSC Adv.*, 2013, **3**, 647; b) M. Wolfs, T. Darmanin and F. Guittard, *Eur. Polym. J.*, 2013, **49**, 2267.
37 T. Darmanin and F. Guittard, *Mater. Chem. Phys.*, 2014, **146**, 6.
38 T. Darmanin, C. Mortier and F. Guittard, *Adv. Mater. Interfaces*, 2014, **1**, 1300094/1.
39 J. P. Giesy, K. Kannan and *Environ. Sci. Technol.*, 2001, **35**, 1339.
40 M. Houde, J. W. Martin, R. J. Letcher, K. R. Solomon and D. C. G. Muir, *Environ. Sci. Technol.*, 2006, **40**, 3463.
41 J. Eastoe, A. Paul, S. Nave, D. C. Steytler, B. H. Robinson, E. Rumsey, M. Thorpe, and R. K. Heenan, *J. Am. Chem. Soc.*, 2001, **123**, 988.
42 A. Mohamed, K. Trickett, S. Y. Chin, S. Cummings, M. Sagisaka, L. Hudson, S. Nave, R. Dyer, S. E. Rogers, R. K. Heenan and J. Eastoe, *Langmuir*, 2010, **26**, 13861.
43 Y. J. Kim, K. H. Park, J.-j. Ha, D. S. Chung, Y.-H. Kim and C. E. Park, *Phys. Chem. Chem. Phys.*, DOI: 10.1039/c4cp00077c.
44 C. Cui, Y. Sun, Z.-G. Zhang, M. Zhang, J. Zhang and Y. Li, *Macromol. Chem. Phys.*, 2012, **213**, 2267.
45 S. P. Mishra, K. Krishnamoorthy, R. Sahoo and A. Kumar, *J. Polym. Sci., Part A: Polym. Chem.*, 2005, **43**, 419.
46 A. J. Guenthner, S. Khombhongse, W. Liu, P. Dayal, D. H. Reneker and T. Kyu, *Macromol. Theory Simul*., 2006, **15**, 87.
47 A. Grinthal, S.H. Kang, A. K Epstein, M. Aizenberg, M. Khan and J. Aizenberg, *Nano Today*, 2011, **7**, 35.
48 X.-F. Wu and Y. A Dzenis, *Nanotechnology*, 2007, **18**, 285702/1.
49 T. S. Kustandi, V. D. Samper, D. K. Yi, W. S. Ng, P. Neuzil and W. Sun *Adv. Funct. Mater.*, 2007, **17**, 2211.
50 R. N. Wenzel, *Ind. Eng. Chem.*, 1936, **28**, 988.
51 A. B. D. Cassie and S. Baxter, *Trans. Faraday Soc.*, 1944, **40**, 546.
52 T. Young, *Philos. Trans. R. Soc. London*, 1805, **95**, 65.
53 a) L. Feng, Y. Zhang, J. Xi, Y. Zhu, N. Wang, F. Xia and L. Jiang, *Langmuir*, 2008, **24**, 4114; b) J. B. K. Law, A. M. H. Ng, A. Y. He and H. Y. Low, *Langmuir*, 2014, **30**, 325.
54 a) S. Choo, H.-J. Choi and H. Lee, *Matter. Lett.*, 2014, **121**, 170; b) D. Sameoto and C. Menon, *Smart Mater. Struct.*, 2010, **19**, 103001/1.
55 a) Q. Cheng, M. Li, Y. Zheng, B. Su, S. Wang and L. Jiang, *Soft Matter*, 2011, **7**, 5948; b) Q. Cheng, M. Li, F. Yang, M. Liu, L. Li, S. Wang and L. Jiang, *Soft Matter*, 2012, **8**, 6740.
56 S. Yang, J. Ju, Y. Qiu, Y. He, X. Wang, S. Dou, K. Liu and L. Jiang, *Small*, 2014, **10**, 294.
57 a) A. Marmur, *Soft Matter*, 2012, **8**, 6867; b) A. Marmur, *Soft Matter*, 2013, **9**, 7900; b) A. Marmur, *Langmuir*, 2003, **19**, 8343.
58 A. Marmur, *Langmuir*, 2008, **24**, 7573.
59 J.-L. Liu, X.-Q. Feng, G. Wang and S.-W. Yu, *J. Phys.: Condens. Matter*, 2007, **19**, 356002/1.
60 a) E. Bormashenko, *Philos. Trans. R. Soc., A*, 2010, **368**, 4695; b) E. Bormashenko, V. Starov, *Colloid Polym. Sci.*, 2013, **291**, 343.